ACS APPLIED MATERIALS & INTERFACES

Research Article

www.acsami.org

Use of Tyrosyl Bolaamphiphile Self-Assembly as a Biochemically Reactive Support for the Creation of Palladium Catalysts

Jinyoung Kwak and Sang-Yup Lee*

Department of Chemical and Biomolecular Engineering, Yonsei University, 50 Yonsei-ro, Seodaemun-gu, Seoul, Korea 120-749

Supporting Information

ABSTRACT: The self-assembly of tyrosine-containing bolaamphiphile was applied as a catalyst support on which palladium (Pd) catalysts were loaded to exploit the biochemical activity of tyrosine. The bolaamphiphile self-assembled to form spherical structures exposing tyrosine moieties on the surface. The phenyl group of tyrosine was then used to create the Pd catalyst on the spherical self-assembly. Silver (Ag) clusters were decorated on the surface, exploiting the reducing function of the phenyl group. These Ag clusters were further applied to create Pd catalysts through the galvanic replacement reaction in the next step. The produced Pd catalyst showed reliable catalytic activity in decomposing dichromate with a pseudo-first-order reaction rate. The reaction rate constant increased proportionally to the Pd loading on the self-assembly support. In addition, as a solid support, the bolaamphiphile self-assembly made catalyst recovery easy, and the recovered Pd catalysts showed consistent activity after several cycles. The experimental results demonstrated that the bolaamphiphile self-assembly is a promising organic support with biochemical activity for the facile creation of metallic catalysts.

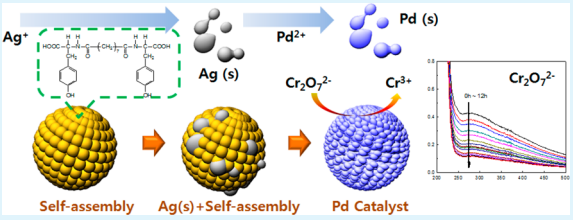

KEYWORDS: *assembly, bolaamphiphile, tyrosine, palladium, catalyst, phenyl*

INTRODUCTION

Palladium (Pd) is an important metallic catalyst that has been widely used in many industrial applications, such as in the Mizoroki−Heck reaction,[1−3] Buchwald−Hartwig reactions,[4,5] Suzuki coupling reaction,[6,7] and other organic coupling reactions.[8] Particularly, colloidal Pd catalysts have attracted research interest because of their versatile uses in aqueous reactions.[9−15] When using a colloidal Pd catalyst, immobilization of Pd clusters on a solid support is required for catalyst recovery and improved efficiency. For these purposes, various catalyst supports have been examined and, specifically, polymeric[16,17] and biological[18−21] supports have attracted research interest because of their extraordinary properties, including their biochemical activity with softness, which differs from conventional inorganic supports such as silica[22,23] and zeolites.[24] Among soft support materials, biological supports are a focus of particular research interest because they have significant advantages compared to other materials. First, the hierarchical complex structure of a biological substance can offer a large surface area with binding sites for catalysts. Second, nucleation and growth of solid catalyst clusters on the biomolecular substance can be regulated through biochemical reactivity. The controlled growth of inorganic clusters by biomolecules offers a new method of catalyst preparation. These two advantages make biomolecular substances attractive reactive catalyst supports. However, the key drawback of biomolecules is their complex preparation in regards to separation and purification, their vulnerability, and the limited affinity of biomolecular substances to metal clusters. One promising method for overcoming these drawbacks is to use biomimetic substances, which possess an ordered structure and biochemical reactivity with a specific affinity to metallic clusters.

Peptidic bolaamphiphilic molecules with a biochemical functional group are a promising biomimetic material that can self-assemble to generate complex structures while maintaining the biochemical activities of the peptide.[25−27] Compared to the common surfactant self-assembly, these peptidic bolaamphiphile assemblies show considerable rigidity and stability like polymeric nanoparticles.[28,29] Thus, the self-assembly of a peptidic bolaamphiphile is applicable as a catalyst support accompanied by chemical reactivity and mechanical strength. Recently, we reported the use of a peptidic bolaamphiphile with tyrosine as a hydrophilic ending group (Tyr-C7 hereafter, Scheme 1a).[30] The Tyr-C7 bolaamphiphile was self-assembled over a wide pH range to produce nanospherical self-assemblies. The spherical self-assembly of Tyr-C7 is stable under various pH conditions such that it can be exploited as a catalyst support with the reactive surface-exposed phenyl group generating solid clusters by metal-ion reduction.

Herein, we report the use of the nanospherical self-assembly of Tyr-C7 as a reactive biomimetic support for the production of Pd catalysts. As presented in the overall reaction procedure shown in Scheme 1b, in the first step, the spherical Tyr-C7 self-assembly was used to deposit silver (Ag) clusters using the reduction function of the tyrosine moiety. These Ag clusters

Received: December 27, 2013
Accepted: April 3, 2014
Published: April 18, 2014

   dx.doi.org/10.1021/am406010a | ACS Appl. Mater. Interfaces 2014, 6, 6461−6468

Scheme 1. (a) Chemical Structure of the Tyrosyl Bolaamphiphilic Molecule (Tyr-C7)[26] and (b) Schematic of the Pd Catalyst Preparation on the Tyr-C7 Self-assembly through Ag-Ion Reduction by Biochemical Reactivity of the Phenyl Group and a Subsequent Galvanic Replacement Reaction

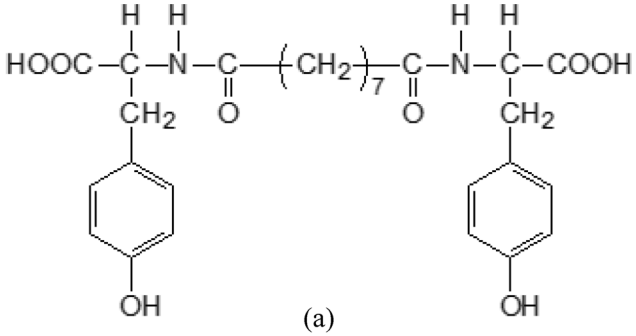

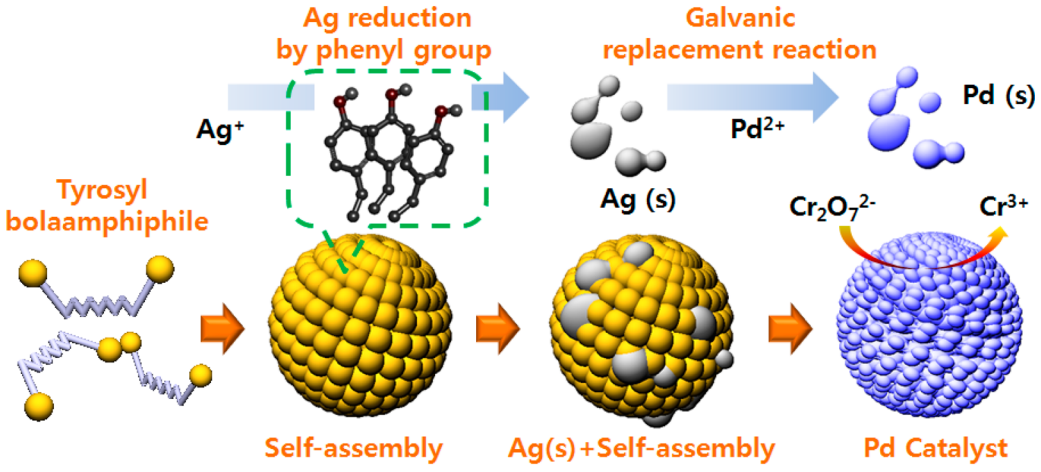

were further exploited as sacrificial substances in the next step for the creation of Pd catalysts through a galvanic replacement reaction. The produced colloidal Pd catalysts were characterized, and their catalytic activity was measured. Studies of the reaction kinetics of the Pd catalyst with decomposition of dichromate proved that the prepared Pd catalyst has reliable catalytic functions even after recycling several times. Furthermore, quantitative analysis of the amounts of Pd precursor and solid Pd catalyst products revealed that the quantity of the loaded Pd catalyst can be minutely tuned by adjusting the reactant concentration. We envision that this biomimetic self-assembly is applicable to the preparation of diverse colloidal catalysts with controlled loading.

EXPERIMENTAL SECTION

Materials. The Tyr-C7 biomimetic bolaamphiphile was synthesized through the carbodiimide conjugation of L-tyrosine-benzylester-*p*-toluenesulfonate and azelaic acid.[30] Silver nitrate ($AgNO_3$; 99%, Sigma-Aldrich) and palladium nitrate [$Pd(NO_3)_2$; 99%, Sigma-Aldrich] were used for the production of Ag clusters and Pd catalysts, respectively. Potassium dichromate ($K_2Cr_2O_7$; 99.5%, Sigma-Aldrich) and sodium formate (HCOONa; 99%, Sigma-Aldrich) were used to prepare the substrate solution for the Pd catalyst. HCl and NaOH (1.0 N each) were used to control the pH. All of the chemicals were used as received.

Synthesis of the Pd Catalyst on Tyr-C7 Self-assembly. The self-assembly of Tyr-C7, which was exploited as a catalyst support, was prepared by simply mixing the synthesized Tyr-C7 powder in a water and methanol mixture (5:1, v/v) at a pH of 6.5 to result in a concentration of 6.7 mM. Nanospherical self-assemblies of Tyr-C7 were obtained instantaneously and used as solid supports for the creation of Pd catalysts. Before Pd catalysts were produced on the Tyr-C7 self-assembly, Ag clusters were deposited, exploiting the activity of the phenyl group. A volume of 1.5 mL of the $AgNO_3$ solution (10 mM) was added to 4.5 mL of the Tyr-C7 self-assembly solution. To promote Ag cluster generation, the solution was adjusted to be basic with a pH of 10.5 and was stirred overnight in the dark. While keeping the solution pH in the range of 10−11, 1.5 mL of a $Pd(NO_3)_2$ solution at various concentrations (5−30 mM) was added to the Ag-decorated Tyr-C7 self-assembly solution. Because of the galvanic replacement reaction of the Ag clusters, the Pd ions were reduced to produce Pd clusters on the Tyr-C7 support. The Pd reaction was also performed in the dark to prevent any photoreaction due to the presence of light. After completion of Ag/Pd deposition, the Pd catalysts on the Tyr-C7 self-assembly support were separated by centrifugation and washed with deionized water three times to remove any chemical residues.

Measurement of the Catalytic Activities and Characterization. The catalytic activity of the prepared Pd catalyst on the Tyr-C7 support was examined by monitoring the reduction of dichromate. Dichromate reduction is a simple reaction carried out in the presence of Pd catalysis in an aqueous solution. An equivolumetric mixture of $K_2Cr_2O_7$ (10 mM) and HCOONa (100 mM) solutions was used as the dichromate substrate whose pH was adjusted to be lower than 3 by the addition of HCl (1.0 N). The reduction experiment was carried out by mixing 2 mL of the dichromate substrate solution and 0.5 mL of the as-prepared Tyr-C7 Pd catalyst solution for 30 min at room temperature. The progress of the dichromate reduction was monitored by measuring the UV absorbance of dichromate at 350 nm using UV/vis spectroscopy (Scinco, Korea, S-3100). After the $Cr_2O_7^{2-}$ reduction experiment, the solid Pd catalysts were collected by centrifugation for the reuse test. The collected catalysts were washed twice with deionized water to remove the remaining chemicals. The washed

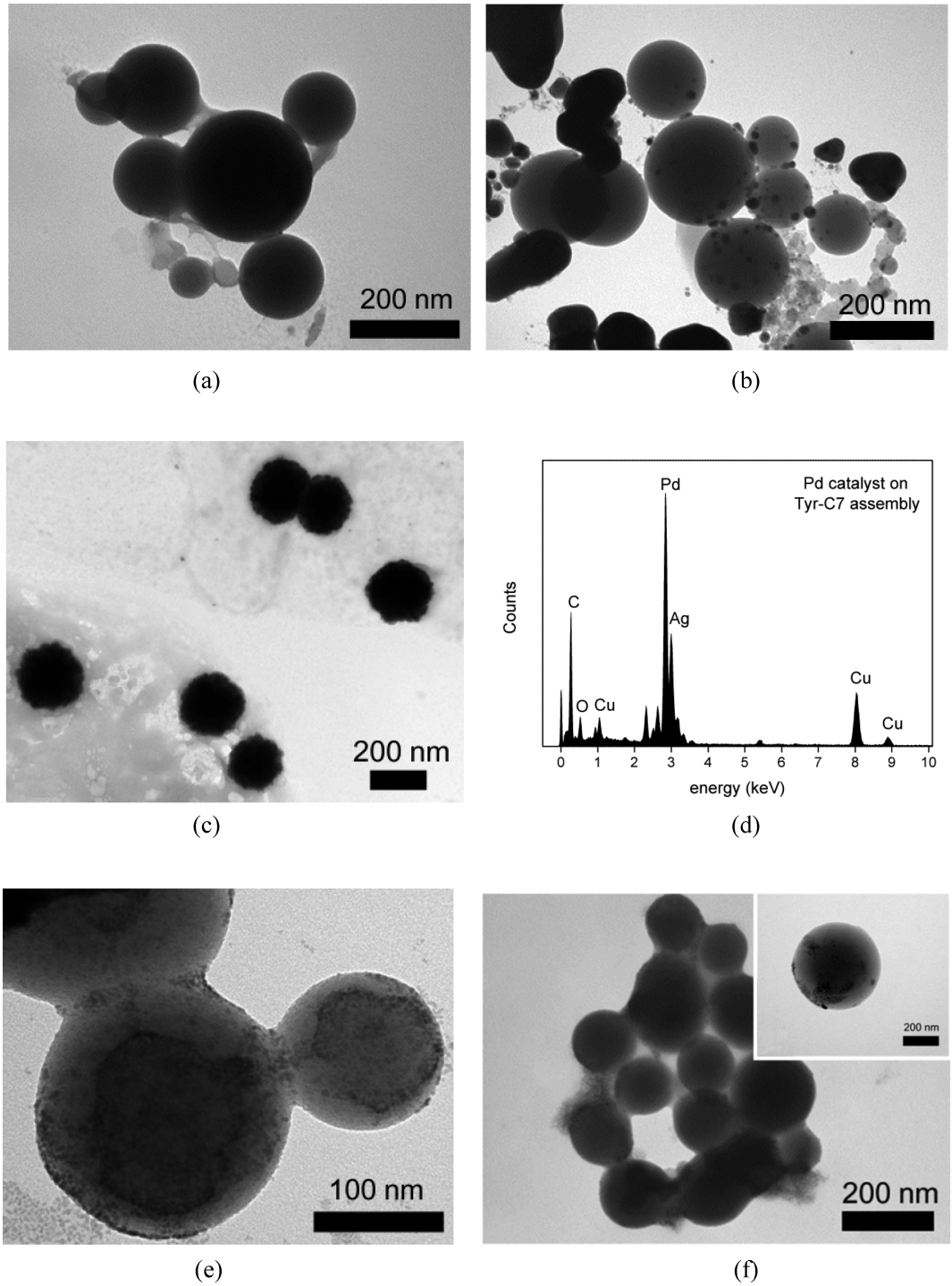

Figure 1. TEM images of Tyr-C7 assemblies with deposited catalytic metal clusters: (a) intact Tyr-C7 spherical self-assembly; (b) Ag-cluster-decorated Tyr-C7 assembly; (c) Pd catalyst on the Tyr-C7 assembly prepared from a 20 mM precursor solution. (d) EDX analysis showing strong Pd and weak Ag traces. (e) Pd clusters on the Tyr-C7 assembly prepared from a 5 mM precursor solution, which incompletely covers the assembly. (f) Pd cluster deposition on the Tyr-C7 assembly without prior Ag deposition where discrete Pd cluster deposition is visible in the magnified image shown in the inset.

catalysts were weighed and applied for another reduction experiment using the same volume of a dichromate solution. The structural and chemical analyses of the Tyr-C7 self-assemblies and Pd catalysts were performed using transmission electron microscopy (TEM; JEOL, Japan, JEM-1011 and JEM-2010) and energy-dispersive X-ray analysis (EDX; Aztek, England), respectively. Quantification of the Pd catalyst loaded on the Tyr-C7 support was carried out through thermogravimetric analysis (TGA; Mettler Toledo, TGA/DSC1).

RESULTS AND DISCUSSION

Creation of the Pd Catalyst on the Tyr-C7 Self-assembly. Creation of the Pd catalyst on the Tyr-C7 self-assembly support was carried out through two-step metallization exploiting the catalytic properties of tyrosine and the Ag clusters. The as-prepared Tyr-C7 self-assemblies had spherical shapes with an average diameter of 197.6 nm (Figure

dx.doi.org/10.1021/am406010a | ACS Appl. Mater. Interfaces 2014, 6, 6461−6468

1a). Size distributions of the as-prepared Tyr-C7 self-assemblies are also shown in the Supporting Information (SI; see Figure S1a). On the surface of these self-assemblies, the phenyl groups of the tyrosine moiety are exposed and promote the reduction of Ag ions. Deprotonated phenyl groups under basic conditions become reactive to reduce Ag ions to solid clusters.[31] Association of the discrete Ag clusters was observed after the Ag-ion reduction (Figure 1b). The discrete deposition of Ag is presumably due to the weak binding strength of tyrosine to the solid Ag clusters, although tyrosine can reduce the Ag ion to solid clusters. Once the solid Ag clusters are detached from the Tyr-C7 self-assembly, they work as nuclei and grow further to create large aggregates. Some large Ag aggregates that were not incorporated with Tyr-C7 self-assemblies were removed by centrifugation before further deposition of the Pd catalyst layer. By exploitation of the Ag clusters on the Tyr-C7 assemblies as sacrificial substances, deposition of the Pd catalyst layer was achieved through the galvanic replacement reaction and subsequent growth of the Pd clusters. Figure 1c shows the spherical Pd catalysts prepared from a 20 mM Pd precursor solution. The average size of the Pd-deposited assemblies increased to 224.8 nm, which is indicative of the self-catalyzing growth of the Pd layer (see the SI, Figure S1b). The Pd clusters generated from the Ag clusters may have functioned as a catalyst, leading to extended growth of Pd. The UV/vis spectrum of the Pd-deposited self-assemblies showed a broad peak at around 310 nm, suggesting the aggregation and growth of Pd clusters (see the SI, Figure S2). EDX analysis of the prepared Pd layer confirmed the presence of traces of Ag and Pd, demonstrating the incorporation of Ag−Pd on the Tyr-C7 assemblies (Figure 1d). High-resolution TEM (HR-TEM) of a catalyst showed that the Pd layer was polycrystalline (see the SI, Figure S3). This polycrystalline structure implies that the Pd layer might be generated by the multiple nucleation and growth of the Pd clusters.

Control experiments were conducted to investigate the effects of the Pd precursor solution and Ag clusters on the creation of Pd catalysts. First, Pd catalyst creation was tested using Pd precursor solutions with concentrations of 5−30 mM. When the 5 mM precursor solution was applied, the Pd clusters partially covered the Tyr-C7 assembly, indicating an insufficient supply of Pd sources for full coverage of the Tyr-C7 assembly (Figure 1e). In contrast, large aggregates of Pd clusters were observed with less coverage on the Tyr-C7 assemblies when the 30 mM solution was applied (data not shown). The production of large aggregates implies that the self-catalytic growth of Pd nanoparticles is prevailing over growth by sacrificial Ag clusters on the surface of the Tyr-C7 assembly at a high Pd-ion concentration. Another control experiment was conducted to confirm the catalytic effect of the Ag clusters. When a 20 mM Pd precursor solution was applied in the absence of Ag clusters, only a small amount of Pd clusters was deposited on the surface of the Tyr-C7 assembly and few Pd aggregates were observed (Figure 1f). This clearly indicates that the Ag clusters promote reduction of the Pd ions to produce solid Pd catalysts, rationalizing the creation of Ag clusters prior to Pd reduction. Considering that the reduction potential of Pd^{2+} (E^0 = +0.99 V) is higher than that of Ag^+ (E^0 = +0.80 V), it is reasonable to presume that fewer Pd clusters are produced solely by the phenyl groups[32] and the reduction of Pd^{2+} ions is achieved by the galvanic replacement reaction. Inhibition of Pd-ion reduction to solid Pd clusters can be explained in view of the electrochemistry with consideration of the tyrosine reduction potential. The reduction potential of tyrosine is approximated to be 0.795 ± 0.005 V in the pH range of 10.5−11.0 according to the literature.[33] Therefore, reduction of the Pd ion will not occur spontaneously because the total reduction potential becomes negative (see eq 1; TyrO* and TyrOH represent the deprotonated and protonated phenyl groups of tyrosine, respectively).

$$2\text{TyrO}^* + \text{Pd}^{2+} \rightarrow 2\text{TyrOH} + \text{Pd(s)} \qquad E^0 = -0.60\ \text{V} \tag{1}$$

On the contrary, the reduction potential of Ag-ion reaction becomes positive, which results in a spontaneous reaction under such basic conditions. The results of the control experiments suggest that the loading of Pd clusters on the Tyr-C7 assembly can be controlled by adjusting the precursor concentration and by proper selection of the catalyst.

The catalytic effect of the Ag clusters on Pd reduction was investigated further through UV/vis spectroscopy. For quantitative analysis, decay of the UV absorbance intensity was monitored as Pd metallization progressed. Figure 2 shows

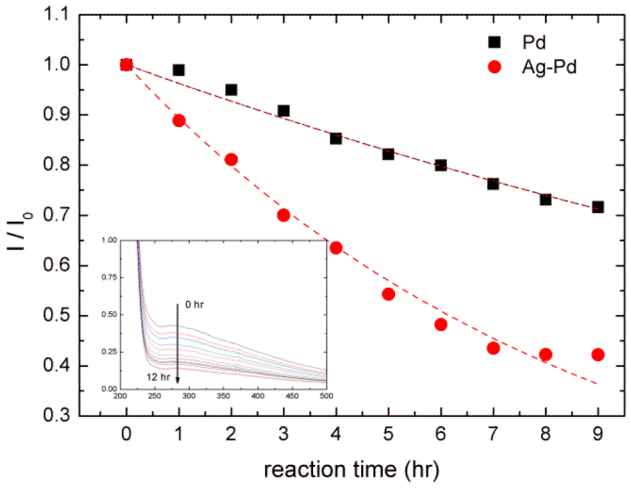

Figure 2. Solid Pd catalyst creation from the precursor solution as a function of time in the presence (red sphere) and absence (black square) of Ag clusters. The inset shows the UV/vis spectra of the Pd precursor obtained as a function of time. The concentration of the Pd precursor solution was determined from the intensity reading at 270 nm.

the decay of the Pd precursor concentration as a function of the progress of metallization in the presence and absence of Ag clusters. The inset in the figure shows the UV/vis spectra as a function of the progress of the reaction. Assuming that Pd^{2+}-ion reduction is a first-order reaction, the UV intensity data were fitted to the exponential decay model shown in eq 2,

$$\frac{I}{I_0} = \exp(-k_1 t) \tag{2}$$

where I_0 and I are the UV absorbance intensities (λ_{abs} = 300 nm) of the Pd precursor obtained initially and as a function of the reaction time, respectively, and k_1 is the kinetic constant (h^{-1}). The estimated kinetic constants of each reaction are 0.1125 and 0.0377 h^{-1}, respectively, indicating 3-times-faster Pd reduction in the presence of Ag clusters. The UV spectroscopy results agree with the TEM observations, demonstrating the promoted Pd reduction by the Ag clusters. It is notable that the Tyr-C7 assembly can also reduce Pd ions, although the rate of

dx.doi.org/10.1021/am406010a | ACS Appl. Mater. Interfaces 2014, 6, 6461−6468

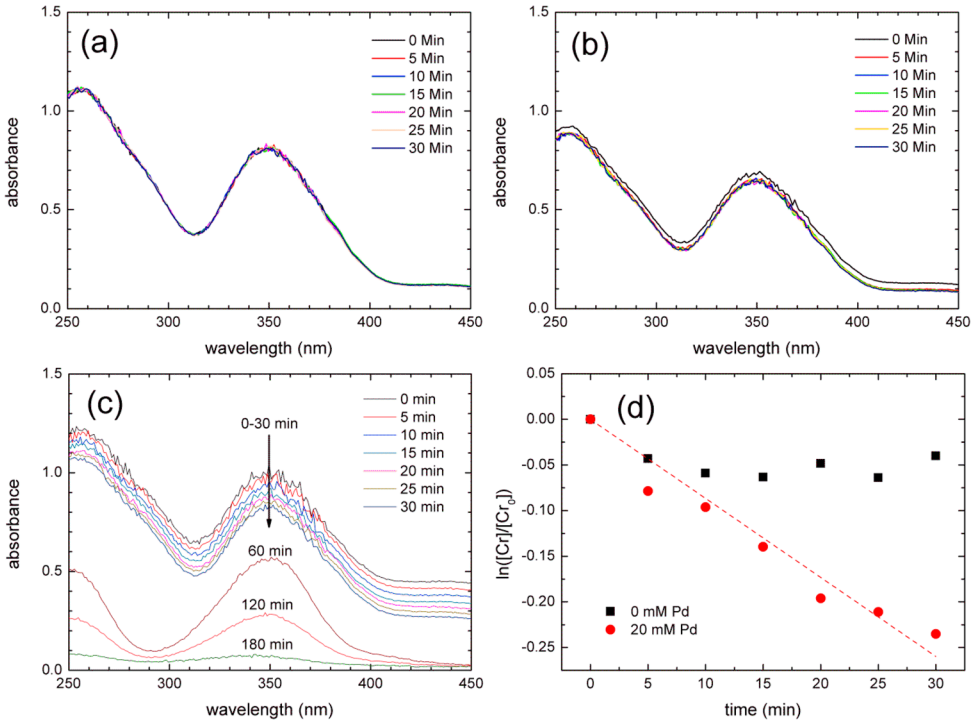

Figure 3. UV/vis spectroscopy results used to monitor the dichromate conversion. (a) No dichromate decomposition was obtained in the presence of the intact Tyr-C7 assembly, as demonstrated by the invariant UV spectra. (b) Slight decomposition of dichromate occurred only at the early stage of the reaction (<5 min) in the presence of Ag clusters on the Tyr-C7 assembly. (c) Fast and continuous decomposition of dichromate occurred in the presence of Pd catalysts on the Tyr-C7 assembly. (d) Decomposition of dichromate over time shows an exponential time dependence in the presence of the Pd catalyst (red circles). Ag clusters did not decompose dichromate (black squares).

reduction is not as significant, while no notable change in the Pd precursor was observed in the absence of the Tyr-C7 assembly (data not shown).

Catalytic Activity of the Tyr-C7 Pd Catalysts. Dichromate reduction was utilized to quantify the catalytic activity of the Tyr-C7 Pd catalysts. The dichromate reduction was carried out in the presence of formate ions and consisted of the two following chemical reactions (3) and (4).[34]

$$Cr_2O_7^{2-} + 14H_3O^+ + 6e^- \leftrightarrow 2Cr^{3+} + 21H_2O \quad (3)$$

$$HCOO^- + H_2O \leftrightarrow CO_2 + H_3O^+ + 2e^- \quad (4)$$

The reduction of dichromate ions ($Cr_2O_7^{2-}$) was mainly achieved by chemical reaction (3), while the formate ions ($HCOO^-$) generated from the dissolution of sodium formate (HCOONa) in an acidic solution were used as the electron donor in reaction (4). When the concentration of formate ions is high enough, the effect of the formate ions is negligible and the dichromate reduction is thought to be governed by reaction (3) only. Therefore, the dichromate reduction reaction can be assumed to be a first-order reaction in regards to the chromate-ion concentration. On the basis of the above assumption, the reaction rate of dichromate reduction can be expressed as shown in eqs 5 and 6.

$$r_{Cr^{6+}} = -\frac{dC_{Cr^{6+}}}{dt} = kC_{Cr^{6+}} \quad (5)$$

$$\ln\left(\frac{C_{Cr^{6+}}}{C_{Cr^{6+},0}}\right) = -kt \quad (6)$$

Here, $r_{Cr^{6+}}$ is the reaction rate of Cr^{6+} ions, $C_{Cr^{6+},0}$ and $C_{Cr^{6+}}$ are the Cr^{6+}-ion concentrations measured initially and at the time of the reaction, respectively, and k is the reaction rate constant (min^{-1}). Using the reaction rate equations listed above, the experimental results were analyzed by plotting $\ln(C_{Cr^{6+}}/C_{Cr^{6+},0})$ against the reaction time, t. The Cr^{6+}-ion concentrations were determined from the calibration curve.

Prior to quantitative analysis, the catalytic activity of the Pd clusters was verified through control experiments. Figure 3 shows the UV spectra of dichromate obtained from the series of control experiments. Figure 3a indicates that there was little change in the dichromate spectra when as-prepared Tyr-C7 assemblies were applied. The characteristic absorbance peak of dichromate at 350 nm did not change with time. This invariance supports the hypothesis that the Tyr-C7 assembly does not influence the dichromate ions or absorb dichromate ions. When Ag clusters existed on the Tyr-C7 assembly, a slight decay of the absorbance was observed only over the first 5 min (Figure 3b). At longer times, little change of the absorbance spectrum was observed. This indicates that the Ag clusters do not reduce the dichromate ions either. The initial decay may be caused by other unknown factors such as residual chemicals or artifacts. Application of the Pd catalyst remarkably reduced the dichromate ions, as shown in Figure 3c. The dichromate peak continually decreased with time, confirming the catalytic function of the Tyr-C7 Pd catalyst. On the basis of the previous reaction rate equation (6), the changes of the logarithm of the dichromate concentration were plotted versus the reaction time. Figure 3d clearly shows that the concentration of dichromate decays exponentially in the presence of the Tyr-C7 Pd catalyst. However, little change was observed for the Ag clusters. This exponential decay

dx.doi.org/10.1021/am406010a | ACS Appl. Mater. Interfaces 2014, 6, 6461−6468

suggests that the pseudo-first-order reaction assumption is suitable for describing the reaction kinetics.

The influence of the Pd concentration on the catalytic activity was investigated through quantitative analysis. The reaction kinetics were evaluated as the Pd precursor concentration was varied, which influences the loading of the solid Pd catalyst on Tyr-C7. Promotion of the dichromate reduction was observed with increasing Pd precursor concentration, as shown in Figure 4a. The reaction rate

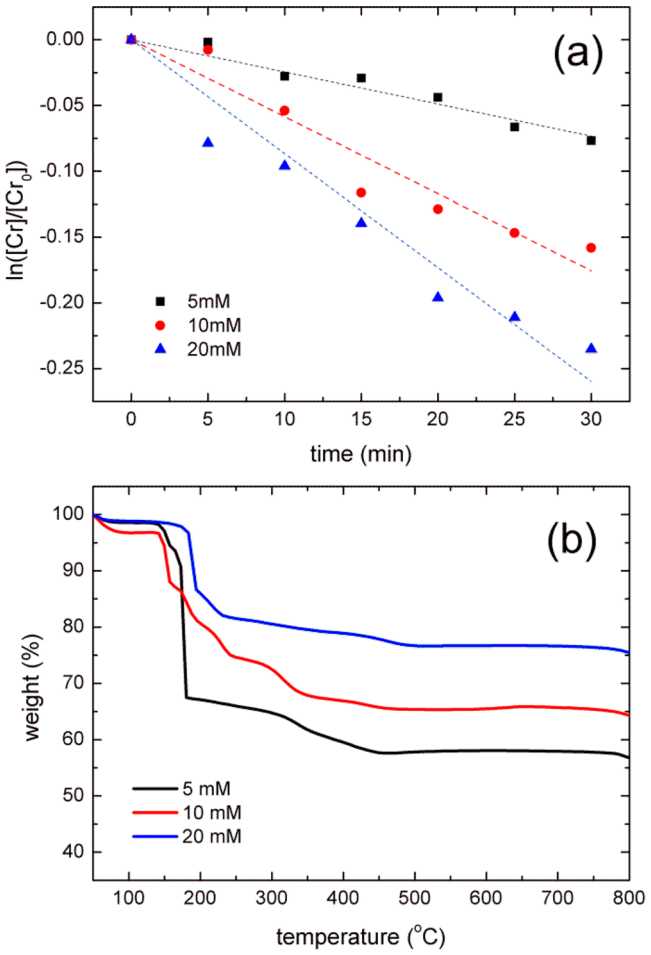

Figure 4. Catalytic activity and production of the solid Pd catalyst as the Pd precursor concentration was varied. (a) Decomposition of dichromate by the Pd catalyst prepared from various precursor concentrations. (b) TGA profiles of Pd catalysts with different metallic contents.

constants, k, were determined from the slopes of each plot and are summarized in Table 1. The rate constant showed a positive correlation with the concentration of the Pd precursor solution, which led to increased production of the Pd catalyst.

Table 1. Reaction Rate Constants (k) and Pd Content of the Tyr-C7 Pd Catalyst

Pd concentration (mM)	solid content (%)	k (min^{-1})	rate constant per solid mass (min^{-1}/g)
5	59	2.44×10^{-3}	0.21
10	70	5.85×10^{-3}	0.41
20	79	8.66×10^{-3}	0.44

TGA of the produced Tyr-C7 Pd catalyst was performed to quantify the amount of created solid Pd clusters. Figure 4b shows the TGA results of each Tyr-C7 Pd catalyst. The TGA profiles clearly indicate that the organic compounds of Tyr-C7 are completely burned out at 450 °C and the solid Pd clusters remain over the temperature range. On the basis of the weight percent of the solid clusters obtained from the TGA data, the solid catalyst loadings for each Tyr-C7 catalyst were calculated and are summarized in Table 1.

Investigation of the Pd content and reaction rate constant revealed that there was a positive correlation between the reaction rate constant and the weight of solid Pd clusters in the experimental range. This positive relationship clearly indicated that more solid Pd catalysts were created and less sacrificial Ag remained with an increase of the Pd concentration. The rate constant per unit mass of Pd clusters of the 5 mM sample was about a half the value obtained from other samples. This is presumably due to the Ag clusters remaining after Pd cluster creation because the 5 mM Pd solution was not concentrated enough to replace all Ag clusters on the self-assembly, leading to the coexistence of Ag and Pd clusters. The remaining Ag clusters would not contribute to catalysis, although their weight was counted in TGA analysis. Although the large Ag aggregates were removed before carrying out the Pd reaction, the 5 mM Pd precursor solution may be insufficient to replace all solid Ag clusters with solid Pd. One potential factor of this incomplete replacement is growth of the solid Pd clusters that were initially generated by the galvanic replacement reaction. Because many Pd ions were consumed for growth of the Pd cluster, not every sacrificial Ag reacted with a Pd ion, resulting in the coexistence of Ag and Pd clusters. When the Pd precursor concentration was increased to 10 mM or higher, the replacement reaction was completely carried out such that few Ag clusters remained on the self-assembly surface. These fully converted Pd clusters resulted in a similar rate constant per unit mass value.

The catalytic performance of the prepared Pd catalyst on the Tyr-C7 self-assembly was compared to that of Pd aggregates prepared without the Tyr-C7 assembly. In the absence of the Tyr-C7 self-assembly, disordered aggregates of Pd clusters were produced by adding a reducing agent of $NaBH_4$ to the precursor solution. The reaction rate constant of the Pd aggregates was 0.67 min^{-1}/g, which is around 1.5-fold higher than that of the Tyr-C7 Pd catalyst. This higher activity is due to the large surface area of the Pd aggregates. Considering that the Pd catalyst on the self-assembly has an ordered spherical structure, the small surface area might result in such differences in the catalytic performance.

Reuse of the Tyr-C7 Pd Catalysts. For practical use of the Tyr-C7 Pd catalyst, the catalytic activities of the reused catalysts were evaluated. Because the Tyr-C7 self-assembly functioned as a support for the Pd clusters, collection of the catalyst was easily achieved after use by microcentrifugation and subsequent washing with deionized water. The weight ratio of the catalyst, which is indicative of the recycle ratio of the catalyst, was reduced to ca. 40% after the first reuse, and then it did not change any more after two reuse cycles (Table 2). This demonstrates stabilization of the Tyr-C7 Pd catalyst after two reuse cycles where Pd clusters presumably bind tightly to the Tyr-C7 support. The decrease of the catalytic activity at the first reuse is presumably due to washing off of the weakly bound Pd clusters from the Tyr-C7 assembly. Some Pd nanoparticles physically adhering to the catalysts might be detached by

Table 2. Weights and Reaction Rate Constants of the Catalyst with Repeated Use

	reuse cycle			
	first	second	third	fourth
catalyst weight ratio, w_i/w_0 (%)[a]	71.20	42.41	41.36	41.36
ratio of the reaction rate constant, k_i/k_0 (%)[a]	70.38	41.57	40.28	40.30
rate constant/catalyst weight (min^{-1}/g)	0.44	0.44	0.44	0.44

[a]The subscripts of 0 and *i* indicate the values measured at the initial and after the *i*th reuse, respectively.

washing. This caused considerable reduction of the catalyst weight ratio after the first reuse.

Figure 5 shows the catalytic decomposition of the dichromate ions with reuse of the Tyr-C7 Pd catalysts.

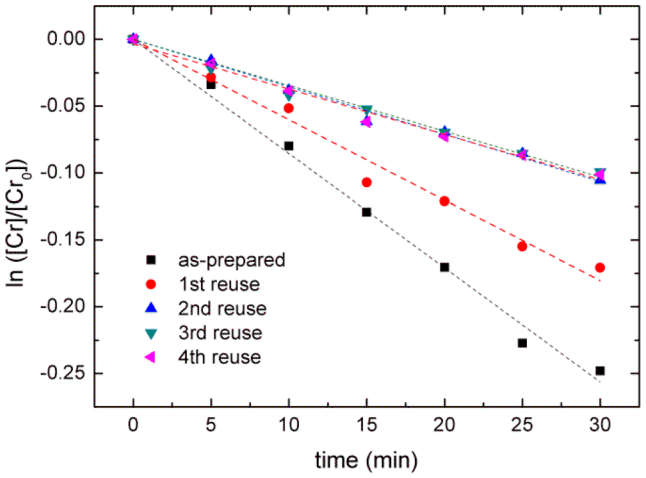

Figure 5. Catalytic activities of the reused Tyr-C7 Pd catalysts where little change in the activity was observed after the second reuse.

Decomposition of the dichromate ions decreased highly at the first reuse; however, it changed little after the second reuse of the catalyst. As shown in Table 2, the ratios of the reaction rate constant were similar to the weight ratios. Thus, the rate constant per unit mass of catalyst changed little during the whole reuse cycles. This consistency of the rate constant per catalyst weight implied that the catalytic property of the Pd cluster was not degraded and that reduction of the reaction rate shown in Figure 5 was mainly induced by the loss of weakly bound Pd clusters.

CONCLUSION

The self-assembly of tyrosyl bolaamphiphile was successfully applied as an active support of Pd catalysts. Upon exploitation of the sacrificial Ag clusters created by the reduction function of the phenyl group in the bolaamphiphilic molecule, the Pd catalyst layer was created on the self-assembly. The controlled catalytic activity and facile reuse of the Tyr-C7 assembly Pd catalyst demonstrated that the bolaamphiphile self-assembly is a promising catalyst support with biochemical activity for various metal reductions. In addition, the catalyst support of the bolaamphiphile self-assembly showed considerable stability during the various physical and chemical processes accompanied by a wide pH variation. We expect that the stability and biochemical reactivity of the bolaamphiphile self-assembly combined with the inorganic catalyst will provide a novel catalysis technique in the future.

ASSOCIATED CONTENT

Supporting Information

Size distribution of as-prepared self-assemblies and Pd catalysts, UV/vis spectra of metal-decorated self-assemblies, and HR-TEM image of the Pd layer. This material is available free of charge via the Internet at http://pubs.acs.org.

AUTHOR INFORMATION

Corresponding Author

*E-mail: leessy@yonsei.ac.kr. Tel: +82-2-2123-5758. Fax: +82-2-312-6401.

Notes

The authors declare no competing financial interest.

ACKNOWLEDGMENTS

This research was supported by the Basic Science Research Program through the National Research Foundation of Korea funded by the Ministry of Education, Science and Technology (Grant 2012R1A1A2008543).

REFERENCES

(1) Mizoroki, T.; Mori, K.; Ozaki, A. Arylation on Olefin with Aryl Iodide Catalyzed by Palladium. *Bull. Chem. Soc. Jpn.* **1971**, *44*, 581.
(2) Heck, R. F.; Nolley, J. P., Jr. Palladium-Catalyzed Vinylic Hydrogen Substitution Reactions with Aryl, Benzyl, and Styryl Halides. *J. Org. Chem.* **1972**, *37*, 2320−2322.
(3) Clark, J. H.; Macquarrie, D. J.; Mubofu, E. B. Preparation of a Novel Silica-Supported Palladium Catalyst and its Use on the Heck Reaction. *Green Chem.* **2000**, *2*, 53−56.
(4) Muci, A. R.; Buchwald, S. L. In *Topics in Current Chemistry*; Miyaura, N., Ed.; Springer-Verlag: Berlin, Germany, 2002; Vol. *219*, pp 131−209.
(5) Culkin, D. A.; Hartwig, J. F. Palladium-Catalyzed α-Arylation of Carbonyl Compounds and Nitriles. *Acc. Chem. Res.* **2003**, *36*, 234−245.
(6) Miyaura, N.; Suzuki, A. Palladium-Catalyzed Cross-Coupling Reactions of Organoboron Compounds. *Chem. Rev.* **1995**, *95*, 2457−2483.
(7) Mubofu, E. B.; Clark, J. H.; Macquarrie, D. J. A Novel Suzuki Reaction System Based on a Supported Palladium Catalyst. *Green Chem.* **2001**, *3*, 23−25.
(8) Littke, A. F.; Fu, G. C. Palladium-Catalyzed Coupling Reactions of Aryl Chlorides. *Angew. Chem., Int. Ed.* **2002**, *41*, 4176−4211.
(9) Li, Y.; Hong, X. M.; Collard, D. M.; El-Sayed, M. A. Suzuki Cross-Coupling Reactions Catalyzed by Palladium Nanoparticles in Aqueous Solution. *Org. Lett.* **2000**, *2*, 2385−2388.
(10) Li, Y.; El-Sayed, M. A. The Effect of Stabilizers on the Catalytic Activity and Stability of Pd Colloidal Nanoparticles in the Suzuki Reactions in Aqueous Solution. *J. Phys. Chem. B* **2001**, *105*, 8938−8943.
(11) Sakurai, H.; Tsukuda, T.; Hirao, T. Pd/C as Reusable Catalyst for the Coupling Reaction of Halophenols and Arylboronic Acids in Aqueous Media. *J. Org. Chem.* **2002**, *67*, 2721−2722.
(12) Wan, Y.; Wang, H.; Zhao, Q.; Klingstedt, M.; Terasaki, O.; Zhao, D. Ordered Mesoporous Pd/Silica-Carbon as a Highly Active Heterogeneous Catalyst for Coupling Reaction of Chlorobenzene in Aqueous Media. *J. Am. Chem. Soc.* **2009**, *131*, 4541−4550.
(13) Wu, S.; Ma, H.; Zhong, Y.; Lei, Z. Biopolymer−Metal Complex Wool−Pd as a Highly Active Heterogeneous Catalyst for Heck Reaction in Aqueous Media. *Tetrahedron* **2011**, *67*, 250−256.
(14) de Jesus, D. M.; Spiro, M. Catalysis by Palladium Nanoparticles in Microemulsions. *Langmuir* **2000**, *16*, 4896−4900.

(15) Gavia, D. J.; Maung, M. S.; Shon, Y.-S. Water-Soluble Pd Nanoparticles Synthesized from ω-Carboxyl-*S*-Alkanethiosulfate Ligand Precursors as Unimolecular Micelle Catalysts. *ACS Appl. Mater. Interfaces* **2013**, *5*, 12432−12440.
(16) Okamoto, K.; Akiyama, R.; Kobayashi, S. Suzuki-Miyaura Coupling Catalyzed by Polymer-Incarcerated Palladium, a Highly Active, Recoverable, and Reusable Pd Catalyst. *Org. Lett.* **2004**, *6*, 1987−1990.
(17) Mecking, S.; Thomann, R.; Frey, H.; Sunder, A. Preparation of Catalytically Active Palladium Nanoclusters in Compartments of Amphiphilic Hyperbranched Polyglycerols. *Macromolecules* **2000**, *33*, 3958−3960.
(18) Manocchi, A. K.; Horelik, N. E.; Lee, B.; Yi, H. Simple, Readily Controllable Palladium Nanoparticle Formation on Surface-Assembled Viral Nanotemplates. *Langmuir* **2010**, *26*, 3670−3677.
(19) Yang, C.; Manocchi, A. K.; Lee, B.; Yi, H. Viral Templated Palladium Nanocatalysts for Dichromate Reduction. *Appl. Catal., B* **2010**, *93*, 282−291.
(20) Yang, C.; Manocchi, A. K.; Lee, B.; Yi, H. Viral-Templated Palladium Nanocatalysts for Suzuki Coupling Reaction. *J. Mater. Chem.* **2011**, *21*, 187−194.
(21) Qu, K.; Wu, Li.; Ren, J.; Qu, X. Natural DNA-Modified Graphene/Pd Nanoparticles as Highly Active Catalyst for Formic Acid Electro-Oxidation and for the Suzuki Reaction. *ACS Appl. Mater. Interfaces* **2012**, *4*, 5001−5009.
(22) Richmond, M. K.; Scott, S. L.; Alper, H. Preparation of New Catalysts by the Immobilization of Palladium(II) Species onto Silica: An Investigation of Their Catalytic Activity for the Cyclization of Aminoalkynes. *J. Am. Chem. Soc.* **2001**, *123*, 10521−10525.
(23) Polshettiwar, V.; Len, C.; Fihri, A. Silica-Supported Palladium: Sustainable Catalysts for Cross-Coupling Reactions. *Coord. Chem. Rev.* **2009**, *253*, 2599−2626.
(24) Okumura, K.; Nota, K.; Yoshida, K.; Niwa, M. Catalytic Performance and Elution of Pd in Heck Reaction over Zeolite-Supported Pd Cluster Catalyst. *J. Catal.* **2005**, *231*, 245−253.
(25) Matsui, H.; Holtman, C. Organic Nanotube Bridge Fabrication by Controlling Molecular Self-assembly Processes between Spherical and Tubular Formations. *Nano Lett.* **2002**, *2*, 887−889.
(26) Kokkoli, E.; Mardilovich, A.; Wedekind, A.; Rexeisen, E. L.; Garg, A.; Craig, J. A. Self-assembly and Applications of Biomimetic and Bioactive Peptide-Amphiphiles. *Soft Matter* **2006**, *2*, 1015−1024.
(27) Spear, R. L.; Tamayev, R.; Fath, K. R.; Banerjee, I. A. Templated Growth of Calcium Phosphate on Tyrosine Derived Microtubules and Their Biocompatibility. *Colloid Surf., B* **2007**, *60*, 158−166.
(28) Kim, J.-K.; Lee, E.; Huang, Z.; Lee, M. Nanorings from the Self-assembly of Amphiphilic Molecular Dumbbells. *J. Am. Chem. Soc.* **2006**, *128*, 14022−14023.
(29) Rösler, A.; Vandermeulen, G. W. M.; Klok, H.-A. Advanced Drug Delivery Devices via Self-assembly of Amphiphilic Block Copolymers. *Adv. Drug Delivery Rev.* **2012**, *64*, 270−279.
(30) Kwak, J.; Park, S.-I.; Lee, S.-Y. Use of the Self-assembly of Tyrosine-Containing Bolaamphiphile Molecules as a Reactive Template for Metal Deposition. *Colloid Surf,. B* **2013**, *102*, 70−75.
(31) Si, S.; Bhattacharjee, R. R.; Banerjee, A.; Mandal, T. K. A Mechanistic and Kinetic Study on the Formation on Metal Nanoparticles by Using Synthetic Tyrosine-Based Oligopeptides. *Chem.—Eur. J.* **2006**, *4*, 1256−1265.
(32) Hayes, P. *Process principles in minerals and materials production*; Hayes Publishing Co.: Cincinnati, OH, 1993.
(33) Harriman, A. Further Comments on the Redox Potentials of Tryptophan and Tyrosine. *J. Phys. Chem., B* **1987**, *91*, 6102−6104.
(34) Vincent, T.; Guibal, E. Chitosan-Supported Palladium Catalyst. 1. Synthesis Procedure. *Ind. Eng. Chem. Res.* **2002**, *41*, 5158−5164.